Sound radiation from a water-loaded cylinder due to machine noise

Xia PAN[1]; Yan TSO[1]; James FORREST[1]; Herwig PETERS[2]

[1]Defence Science and Technology Organisation, Australia

[2]The University of New South Wales, Australia

ABSTRACT

This paper presents the modelling and analysis of the noise radiation due to internal acoustic excitation of a cylinder submerged in a heavy fluid. The cylinder consists of a cylindrical shell filled with air and attached to rigid end plates. The acoustic excitation is modelled as monopoles to simulate the operation of a machine noise source in the cylindrical shell. In order to model the noise transmission and radiation, the machine noise is characterised as multiple monopole sources with random amplitudes and random phases on the surfaces of an imaginary component boundary. An initial study including the effect of absorbing material on noise radiation is presented. Some of the analytical results are compared with those from numerical finite element / boundary element models. Excellent agreement is obtained between the analytical results and results from the numerical method.

Keywords: Machine Noise, Absorbing Material, Under Water Acoustics
I-INCE Classification of Subjects Number(s): 54.3

1. INTRODUCTION

Water-loaded cylindrical enclosures are widely used as simple examples to demonstrate the acoustic characteristics of underwater vessels. This preliminary study analytically and numerically investigates the transmission and radiation of internal machine noise from a cylindrical enclosure through modelling. To model the machine noise, the acoustic emission may be characterised as a component source, with transfer functions developed to represent the acoustic radiation.

Sound radiation from a water-loaded vibrating cylindrical shell can be modelled using the following three steps. The first step is to model a finite shell. Detailed discussions and comparisons of different shell equations were given by Pan and Hansen (1). The second step is to model the excitation. The expression for a point force acting on a shell has been widely reported (see, for example, Pan and Hansen (1) and Pan *et al.* (2, 3)). An approximate solution for a single monopole source inside a shell was given by James (4). This solution has been validated by Pan *et al.* (5) where good agreement was obtained between the analytical results and results from numerical finite element/boundary element (FE/BE) models. The third step is to model the sound radiation from the shell. An approximation for sound radiation from a vibrating shell was given by Junger and Feit (6), Tso and Jenkins (7) and Pan *et al.* (5).

In practice, a machine has a finite size and the enclosure, in some cases, contains some absorption material on the internal wall. The first part of the current work is to extend the previous theory on the monopole excitation in Ref. (5) to machine noise. To the authors' knowledge, this work has not been addressed previously. The second part of the current work is to model the effect of absorbing material on noise radiation.

The classical description of sound absorption in a diffuse sound field in an enclosure is based on the Sabine theory which is given in texts such as Bies and Hansen (8). The Sabine absorption coefficient represents the average fraction of incident energy absorbed. The sound decay rate depends on the absorption coefficient, the enclosure volume and wall area, and the sound speed. The absorption coefficient may be obtained by measurement of a layer of absorption material on the internal wall of the enclosure. However, the absorption coefficient is difficult to incorporate into the current analytical model. This paper describes an approximate approach to convert the absorption coefficient into the loss factor of the sound speed in the enclosure. Thus, the effect of absorbing material can be easily included in the current model.

2. ANALYTICAL METHOD

A finite cylindrical shell model for calculating the far-field pressure, developed by Junger and Feit (6) and later used by Tso and Jenkins (7) and Pan *et al.* (5), is shown in Figure 1(a). The cylindrical shell has two rigid end plates (to form a finite cylinder) attached to two semi-infinite rigid baffles, so that there is no radiated pressure from the end plates. Figure 1(b) shows the cross-section of the shell with an interior monopole source. In figures 1(a) and 1(b), *a* is the radius, *h* is the thickness, *L* is the half-length of the shell and r_0 is the radial distance between the source and the z-axis. All symbols used are defined in the nomenclature at the end of the paper. The representation of the machine noise source as an equivalent box source is shown in Figure 2. This noise source is modelled as a number of monopole sources spread over the corners and faces of the box.

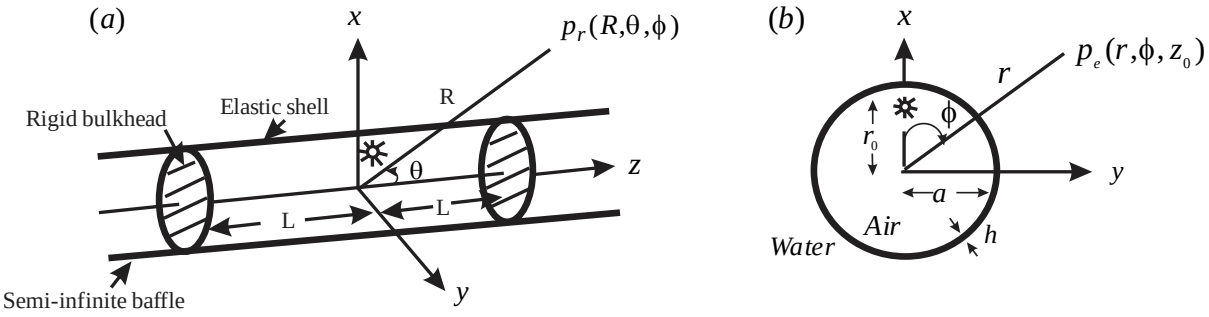

Figure 1 – Geometry and coordinate systems of a cylindrical shell: (a) finite cylindrical shell with semi-infinite baffles; (b) cross-section of shell with a monopole source.

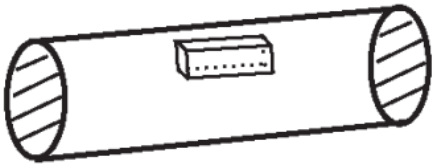

Figure 2 – Finite cylinder with machine noise

2.1 Shell Dynamics

The shell equations used in this paper were given by Junger and Feit (6), who developed the Donnell formulation to include water loading for a thin shell. The water loading of the shell was obtained by including the acoustic impedance in the formulation. When compared to other thin-shell theory such as Flügge (9), the Donnell formulation has fewer terms, which may underestimate the effect of bending. However, it was judged that the Donnell formulation is sufficient for the purpose of demonstrating the methodology in the modelling of sound radiation due to an acoustic source.

The spectral displacements (modal amplitudes) of a submerged shell at a particular mode are obtained from the following matrix equation:

$$\begin{bmatrix} S_{11} & S_{12} & S_{13} \\ S_{21} & S_{22} & S_{23} \\ S_{31} & S_{32} & S_{33} \end{bmatrix} \begin{bmatrix} U_{mn} \\ V_{mn} \\ W_{mn} \end{bmatrix} = \begin{bmatrix} 0 \\ 0 \\ F_{mn} \end{bmatrix} \tag{1}$$

where the elements shown in the first matrix were defined by Pan *et al.* (5). In Equation (1), U_{mn}, V_{mn} and W_{mn} are the spectral displacements in the axial, circumferential and radial directions of the shell, *m* and *n* are the axial and circumferential mode numbers and F_{mn} is the modal force which describes the type and position of an excitation. The time-harmonic factor $e^{-i\omega t}$ is omitted throughout.

The shell has shear diaphragm or "simply supported" end conditions. The far-field radiated pressure from the shell is determined by the radial displacement. Therefore, only the radial displacement will be presented here. It can be written as a double Fourier series:

$$W(\phi,z)=\sum_{m=1}^{\infty}\sum_{n=1}^{\infty}W_{mn}\sin\left[\frac{m\pi(z+L)}{2L}\right]\cos(n\phi) \tag{2}$$

where W_{mn} may be obtained from Equation (1).

2.2 Excitation

Pan *et al*. (5) showed that the excitation due to a monopole source inside a shell can be determined by the internal pressure p_i. The excitation stress of the shell due to an internal pressure p_i is simply

$$F(\phi,z)=p_i(a,\phi,z). \tag{3}$$

The modal forces F_{mn} are the coefficients of the Fourier series expansion of the force excitation *F*. The expression of the modal force due to multiple monopole sources located inside the cylinder is given by Pan *et al*. (5):

$$F_{mn}=\sum_{q=0}^{\infty}\frac{e_n e_q}{L\gamma_q a}\sum_{s=1}^{j}P_{0s}\cos\left[\frac{q\pi(z_s+L)}{2L}\right]\frac{2m[1-(-1)^{m+q}]}{\pi(m^2-q^2)}\frac{J_n(\gamma_q r_s)}{J_n^{'}(\gamma_q a)} \tag{4}$$

where P_{os} is the complex amplitude of the *s*th source, *j* is the number of the monopole sources at positions $(r_s, z_s, s=1,...,j)$. Complex source amplitudes allow for multiple sources with random amplitudes and random phases.

2.3 Far-field Pressure

Based on the expression for the pressure radiated from a vibrating shell to the far field (Ref. (5)), the pressure due to multiple sources can be expressed as:

$$p_r(R,\theta,\phi)=-i\omega\rho_e c_e\frac{e^{ik_e R}}{\pi R}\sum_{s=1}^{j}\sum_{m=1}^{\infty}\sum_{n=0}^{\infty}\frac{G_{mn}(\alpha)e^{-\frac{in\pi}{2}}}{\sin\theta\cdot H_n^{'}(k_e a\sin\theta)}\cos(n\phi-\phi_{os}) \tag{5}$$

where

$$G_{mn}(\alpha)=LW_{mn}e^{i\alpha L}\frac{m\pi}{2L^2}\cdot\frac{1-(-1)^m e^{-2i\alpha L}}{\left(\frac{m\pi}{2L}\right)^2-\alpha^2}\quad\text{and}\quad\alpha=k_e\cos\theta. \tag{6}$$

The radiated pressure from the shell due to multiple random monopoles can be obtained by substituting the modal force from Equation (4) into Equation (1) to determine W_{mn}, and then using Equations (5) and (6) to solve G_{mn} and $P_r(R,\theta,\phi)$ respectively.

2.4 Sound Absorption

The absorption coefficient is the fraction of incident energy which is absorbed at a surface containing the absorbing material of a reverberant room. Absorption coefficients for some commonly used materials were given by Bies and Hansen (8). As the effect of sound absorption is difficult to incorporate into the current analytical model, an approximation approach is adopted here by assigning the effect of sound absorption to acoustic damping in the enclosure. The acoustic damping is modelled as a loss factor term in the speed of sound in the enclosure.

The speed of sound for a fluid is defined by Ref. (8):

$$c=\sqrt{\frac{K}{\rho}} \tag{7}$$

where K is the bulk modulus and ρ is the density. Equation (7) implies that damping can be included in the speed of sound via the bulk modulus K by using a complex modulus,

$$K^* = K(1 - i\eta_K) \tag{8}$$

where η_K is a damping loss factor. The damped sound speed is obtained by replacing K^* with K in Equation (7) as:

$$c^* = \sqrt{\frac{K^*}{\rho}} = c\sqrt{1 - i\eta_K} \approx c(1 - i\frac{\eta_K}{2}) = c(1 - i\eta_i) \tag{9}$$

where $\eta_i = \eta_K / 2$ is the acoustic damping.

Equivalent measures of damping near a modal resonance frequency are (Ref. (8)):

$$\frac{\Delta f}{f} = \eta_K = \frac{\delta}{\pi} \tag{10}$$

where Δf is the 3 dB bandwidth, f is the resonance frequency and δ is the logarithmic decrement. The logarithmic decrement is defined in Ref. (8):

$$\delta = \frac{1}{n}\log_e\left(\frac{A_0}{A_n}\right) = \pi\eta_K \tag{11}$$

where A_0 is the initial amplitude of the oscillating system and A_n is its amplitude n cycles later. Based on the Sabine absorption model, the decay equation of mean squared pressure $\langle p^2 \rangle$ in a reverberant sound field averaging over the modes in a band is given by Ref. (8):

$$\langle p^2 \rangle = \langle p_0{}^2 \rangle e^{-Sc\bar{\alpha}t/4V} \tag{12}$$

where $\langle p_0{}^2 \rangle$ is the initial mean squared pressure, S is the surface area, $\bar{\alpha}$ is the absorption coefficient and V is the enclosure volume. Using the definition of one period $T = 1/f = 2\pi/\omega$, the pressure amplitudes at $t_0 = 0$ and $t_1 = 2\pi/\omega$ are given by:

$$A_0 = (e^{-Sc\bar{\alpha}t_0/4V})^{1/2} = 1, \tag{13a}$$

$$A_1 = (e^{-Sc\bar{\alpha}t_1/4V})^{1/2} = e^{-Sc\bar{\alpha}\pi/4V\omega}. \tag{13b}$$

Setting $n = 1$ in Equation (11), the logarithmic decrement may be related to the absorption coefficient as:

$$\delta = \log_e\left(\frac{1}{e^{-Sc\bar{\alpha}\pi/4V\omega}}\right) = \frac{Sc\bar{\alpha}\pi}{4V\omega}. \tag{14}$$

Substituting Equation (14) into Equation (11) gives the expression for the damping

$$\eta_K = \frac{\delta}{\pi} = \frac{Sc\bar{\alpha}}{4V\omega}. \tag{15}$$

Note that $\bar{\alpha}$ itself varies with frequency. As an approximation, an average value of η_K over an octave band of band centre frequency ω is used in the present study. Using the definition $\eta_i = \eta_K / 2$, the relationship between acoustic damping and absorption coefficient is given by:

$$\eta_i = \frac{Sc\bar{\alpha}}{8V\omega}. \tag{16}$$

Equation (16) enables the effect of sound absorption materials in the cylindrical shell to be modelled as a loss factor term in the speed of sound according to Equation (9).

3. NUMERIAL METHOD

For validation of the analytical method, a fully coupled FE/BE model (Ref. (5)) was developed where the FEM was used to model the cylindrical shell and the BEM was used to model the interior and exterior fluid domains. The software package ANSYS was used to build the FE model and the code AKUSTA was used to generate the BE model. The approach is described in more detail in Ref. (5). The cylindrical shell and the flat end plates have been discretized using 2240 quadratic finite elements. The internal fluid has been modelled using 496 linear boundary elements and the external fluid has been modelled using 576 linear boundary elements. Two source configurations with equal source strengths were considered:

1. A single acoustic monopole with a surface pressure of 1 Pa applied to a 1 m radius sphere. Note, that the sphere is not actually modelled, the radius is only required to determine the source strength;
2. 14 acoustic monopoles distributed over an imaginary surface of a box with dimensions $0.5\times0.3\times1.0$ m (1 m box) and $0.5\times0.3\times2.0$ m (2 m box). The source strengths were assigned randomly to the monopole sources with the total source strength being equal to that of configuration 1. The 14 equivalent sources were located at the 8 corners and the central points of the 6 surfaces of the imaginary machine boundary.

4. RESULTS

The results presented in this paper are based on the cylindrical shell with the geometric and material properties and excitations shown in Table 1. The maximum mode numbers used in the analytical method are also included in Table 1.

Table 1 – Shell and fluid parameters, and excitations

Steel shell	$E = 1.95\times10^{11}$ N/m^2, $\sigma = 0.29$, $\rho_s = 7700$ kg/m^2, $a = 1.0$ m, $h = 0.01$m, $2L = 10.0$ m (shell length), $2L = 10.0$ m (shell length)
Exterior fluid	$\rho_e = 1000$ kg/m^3, $c_e = 1500$ m/s (water)
Interior fluid	$\rho_i = 1.21$kg/m^3, $c_i = 343.0$ m/s (air)
Monopole source	$P_0 = 1$ Pa, $(r,\phi,z) = (0,0,0)$ (centre), $(r,\phi,z) = (2a/3,0,0)$ (off-axis)
Machine source	$\sum_{s=1}^{14} P_{os} = 1$ Pa, $w_m = 0.3$m (width of box), $h_m = 0.5$ m (height of box), $2l_m = 1$m (length of 1 m box), $2l_m = 2$ m (length of 2 m box), $(r,\phi,z) = (0,0,0)$ (centre), $(r,\phi,z) = (2a/3,0,0)$ (off-axis)
Maximum mode numbers	axial modes: 9, circumferential modes:10, acoustical modes: 20

In Table 1, the monopole source and the centre of the machine/box source are at the origin of the coordinate system or slightly shifted from the origin to $(r,\phi,z) = (2a/3,0,0)$. The latter position of the source is to excite both axisymmetric and non-axisymmetric modes. These sources are named as the central excitation and off-axis excitation respectively. Damping in the shell wall is included by using a complex representation of the Young's modulus $E^* = E(1-i\eta)$ where η is the loss factor and has a

value of 0.02. The sound pressure was calculated at 1000 m with $\theta = 90°$ and $\phi = 0°$, and normalised to 1 m range by adding 60 dB. The dB reference level is 1 μPa.

4.1 Analytical Results

The machine noise in the analytical model was simulated as described in configuration 2 for the numerical approach (see Section 3). For an initial comparison, the analytical results due to a central excitation are presented. Figure 3 shows the comparisons of the radiated pressure due to one monopole source and those due to 14 equivalent sources in-phase or with random phases. The sharp peaks occur at frequencies which correspond to the natural frequencies of the interior enclosure with rigid boundaries, while some less significant peaks correspond to the resonances of acoustically efficient shell modes. Results shown in Figure 3 indicate the radiated pressure due to one monopole source is in good agreement with that of the 14 in-phase sources at frequencies where the internal acoustic wave length is larger than the diameter of the shell ($\lambda_i > 2a$) and the spacing of the monopole sources. These frequencies are below 171 Hz for the current shell dimensions. Here, the shell acts as a one dimensional waveguide. At and above 171 Hz ($\lambda_i \leq 2a$), cross modes occur inside the enclosure. The response to the multiple sources then becomes more complex.

It is noticed the radiated pressure due to one monopole source is much higher than that of the 14 random phased sources below 171 Hz. This is because the 14 sources with random phases can cancel out with each other if they are out of phase. The peaks at 20 Hz shown in the green lines (random phase sources) in Figures 3(a) and 3(b) are the acoustic modes which are also present when the off-axis excitation is applied (see Figure 4). Above 171 Hz, the responses of the multiple sources become more complex due to source interactions.

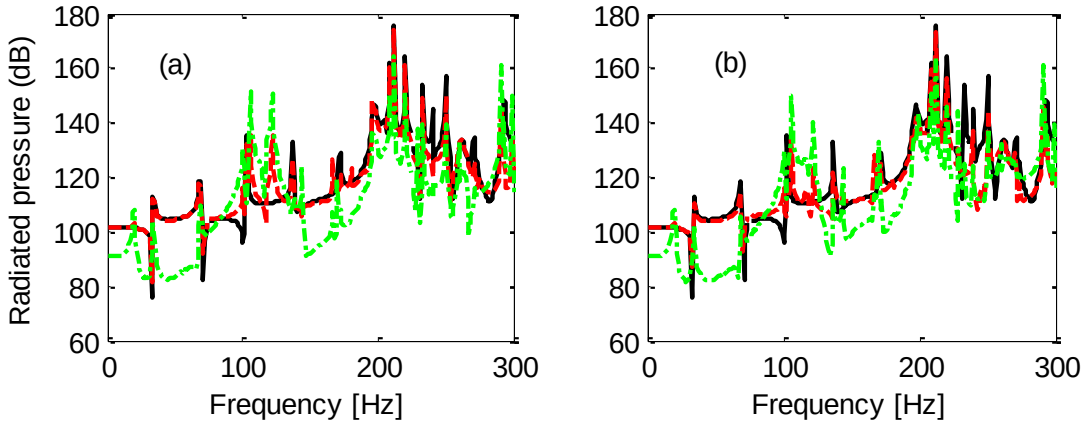

Figure 3 – Far-field radiated pressure from a water-loaded shell due to the central excitation of a monopole or multiple sources located on a box from the analytical method: (a) compared with 1 m box; (b) compared with 2 m box. ─, one monopole; - - -, 14 equivalent sources in-phase; ─ · ─, 14 equivalent sources with random phases.

Figure 4 presents the results for the off-axis excitations. The modal responses of the shell are quite different from those shown in Figure 3 since the off-axis source excites the non-axisymmetric modes in the enclosure and on the shell, notably the mode at 20 Hz which is also excited by the random phase, centrally excited sources.

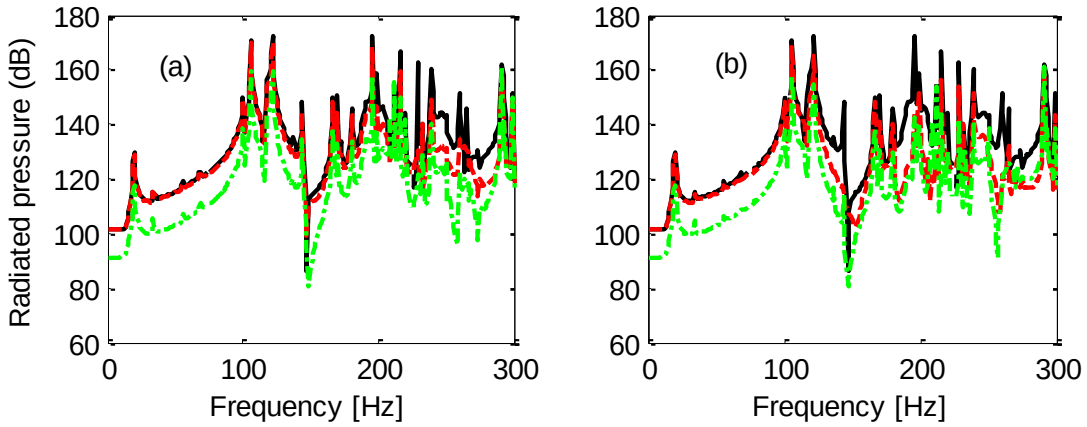

Figure 4 – Far-field radiated pressure from a water-loaded shell due to the off-axis excitation of a monopole or multiple sources located on a box from the analytical method: (a) compared with 1 m box; (b) compared with 2 m box. ─, one monopole; - - -, 14 equivalent sources in-phase; ─ · ─, 14 equivalent sources with random phases.

The results shown in Figures 3 and 4 indicate that the single monopole representation may be used to model multiple in-phase monopole sources below 171Hz. It follows that if the machine noise source is dominated by in-phase excitations at this frequency range, then the machine noise may be modelled by a single monopole. Above 171 Hz, it appears that a single monopole source may overestimate the radiated pressure and the multiple sources representation (either in phase or random phase) may be a more realistic modelling approach.

In what follows, the effect of absorbing material on radiated pressure is presented briefly. Acoustic damping is applied to the interior of the enclosure. As an example, the acoustic damping that is equivalent to 25 mm fibreglass is used to model the speed of sound of the fluid medium in the enclosure. This is implemented by using the acoustic damping value which is equivalent to the absorption coefficient of the fibreglass (see Equation (16)). A single average acoustic damping η_i is calculated for the entire octave band. Damping values of $\eta_i = 0.019$ from an absorption coefficient $\bar{\alpha} = 0.18$ for frequencies below 176 Hz, and $\eta_i = 0.013$ from $\bar{\alpha} = 0.24$ for frequencies from 177 Hz to 300 Hz are calculated (based on values in Ref. (8)). Only the off-axis results are presented in this section.

Figure 5(a) shows the radiated pressure from the shell, with and without a layer of 25 mm fibreglass, due to 14 equivalent in-phase sources located on the 1 m box. Figure 5(b) shows the corresponding results for the 14 equivalent sources with random phases located on the 1 m box. Results show that there is no significant effect at low frequencies with the layer of fibreglass attached. At low frequencies, the acoustic energy passes through the shell without absorption. At high frequencies, an attenuation of 15 dB to 30 dB of the acoustic modes can be observed. It is expected that the layer of fibreglass will have negligible effect on the structural modes. Similar results can be observed for the 14 equivalent sources located on the 2 m box (Figures 5(c) and 5(d)).

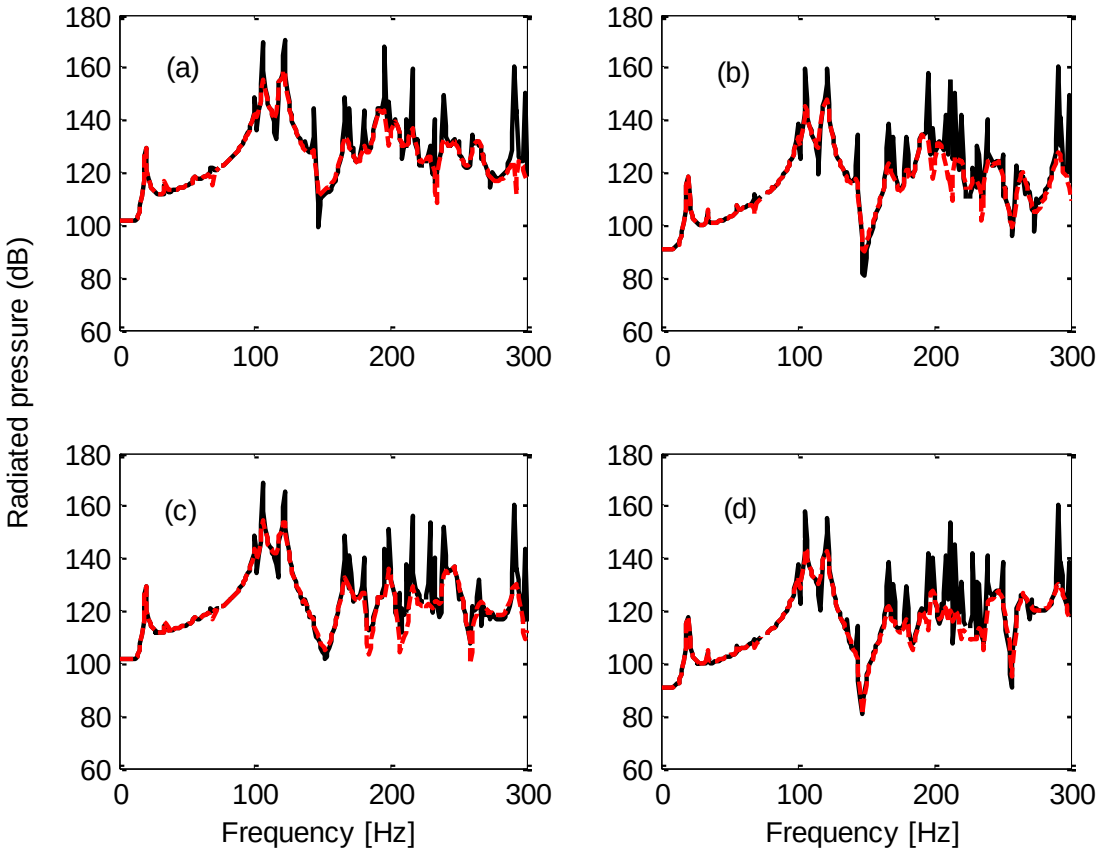

Figure 5 – Far-field radiated pressure from a water-loaded shell due to off-axis excitations with and without a fibreglass layer on the internal wall from the analytical method: (a) due to 14 equivalent in-phase sources located on 1 m box; (b) due to 14 equivalent random phase sources located on 1 m box; (c) due to 14 equivalent in-phase sources located on 2 m box; (d) due to 14 equivalent random phase sources located on 2 m box. ─, without fibreglass; - - -, with fibreglass.

4.2 Comparison with Numerical Results

In this Section, the fully coupled FE/BE method described in Section 3 is used to verify the analytical results. Only the numerical results for 14 equivalent, in-phase sources located on the imaginary box are available and will be compared with those obtained from the analytical model.

Figures 6(a) and 6(b) show the results of radiated pressures due to the central excitation for the two methods. There are some discrepancies in both amplitudes and resonant modes. They are believed to be mainly due to the different boundary conditions in the analytical and numerical methods. Specifically, the numerical model had constraints on the three translational directions at the ends of the shell, where the analytical model had constraints only in the radial and circumferential directions and no constraint in the axial direction at the ends.

Figures 6(c) and 6(d) show the corresponding results for the off-axis excitation. Results shown in Figures 6(c) and 6(d) indicate better agreement between the two methods compared with the centrally excited cases. This may be due to non-axisymmetric modes which are less affected by the difference in boundary conditions.

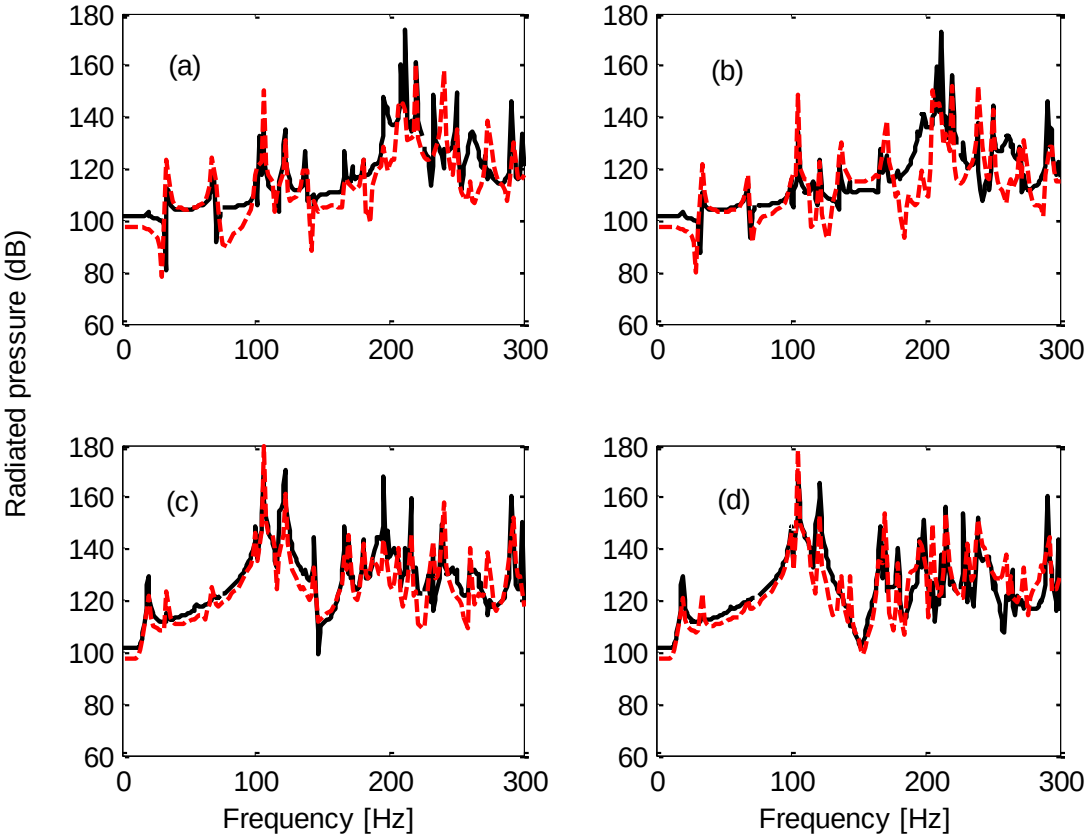

Figure 6 – Far-field radiated pressure from a water-loaded shell due to the excitation: (a) 14 equivalent in-phase sources located on 1 m box at the centre; (b) 14 equivalent in-phase sources located on 2 m box at the centre; (c) 14 equivalent in-phase sources located on 1 m box off-axis; (d) 14 equivalent in-phase sources located on 2 m box off-axis. ─, from the analytical method; - - -, from the coupled FE/BE method.

5. CONCLUSIONS

An analytical method has been developed for predicting far-field sound radiation from a water-loaded finite cylindrical shell excited by interior machine noise. The machine noise was characterised as multiple monopoles with random amplitudes and either in-phase or with random phases located on an imaginary machine boundary. The results in radiated pressure show the dominance of acoustic resonance modes in the enclosure. A single monopole source was also used for the modelling of machine noise for comparison. The results demonstrate that the single monopole source representation may be used to model machine noise at frequencies where the acoustic wave length is larger than the diameter of the shell and the spacing of the monopole sources. Above this frequency range, the radiation due to the machine noise is more complex and the single monopole source may overestimate the radiated pressure due to the geometry and the interactions between the radiators of the machine. It was found that the phases of the radiators significantly changed the amplitude of the sound radiation. Increasing the machine size only slightly decreases the radiated pressure at some high frequencies for the current source configurations.

An initial study including the effect of absorbing material on noise radiation is presented. The results indicate that the absorbing material significantly dampens the acoustic modes in the enclosure at high frequencies, and the attenuation in radiated pressure increases as frequency increases. However, the absorbing material has negligible effect on structural modes.

Validations of the analytical method are presented for some cases by using the fully coupled FE/BE method. Good agreement is obtained between the two methods.

ACKNOWLEDGEMENTS

The authors would like to thank Dr Ian MacGillivray and Dr Nicole Kessissoglou for their useful discussions and suggestions.

REFERENCES

1. Pan X, Hansen CH. Active control of vibration transmission in a cylindrical shell. JSV. 1997; 203(3):409-434.
2. Pan X, Tso Y, Juniper R. Active control of low-frequency hull-radiated noise. JSV. 2008a;313:29-45.
3. Pan X, Tso Y, Juniper R. Active control of radiated pressure of a submarine hull. JSV. 2008b;311:224-242.
4. James JH. An approximation from a simply-supported cylindrical shell excited by an interior point source. Admiralty Marine Technology Establishment, Teddington, AMTE(N) TM85024. 1985.
5. Pan X, MacGillivray I, Tso Y, Peters H. Investigation of sound radiation from a water-loaded cylindrical enclosure due to airborne noise. Proc Acoustics 2013, Victor Harbor, Australia 2013.
6. Junger MC, Feit D. Sound, Structures, and Their Interaction. The MIT Press Classic, Boston; 1986. 16–312.
7. Tso YK, Jenkins CJ. Low frequency hull radiation noise. Report No. Dstl/TR05660, Defence Science and Technology Laboratory, UK; 2003.
8. Bies DA, Hansen CH. Engineering Noise Control-Theory and Practice. 2nd ed. E & FN Spon, London; 1996. 230-430.
9. Flügge W. Stresses in Shells. Springer-Verlag, Berlin; 1973. 204–259.

NOMENCLATURE

a	radius of cylindrical shell	s	index number
A	amplitude of vibrating system	S	surface area
c	sound speed	t	time
K	bulk modulus	U_{mn}	spectral axial displacement
E	Young's modulus	V	volume
e_n	$=1$ for $n=0$ and $e_n=2$ for $n>0$	V_{mn}	spectral circumferential displacement
e_q	$=1$ for $q=0$ and $e_q=2$ for $q>0$	W	radial displacement
f	3 dB bandwidth frequency	w_m	width of machine
F	excitation stress	W_{mn}	spectral radial displacement
F_{mn}	modal force	$\overline{\alpha}$	absorption coefficient
h	thickness of shell	δ	logarithmic decrement
h_m	height of machine	γ_q	$=(k_i^2-q^2\pi^2/4L^2)^{1/2}$
H_n	Hankel function of order n	η	$=0.02$ (structural loss factor)
i	$=\sqrt{-1}$ (complex unit)	η_i	interior loss factor of sound
j	number of monopole sources	η_K	loss factor in K
J_n	Bessel function of order n	ρ	mass density
k	ω/c (wave number)	ω	circular frequency
L	half-length of cylindrical shell	(x,y,z)	Cartesian coordinates
l_m	half- length of machine	(r,ϕ,z)	cylindrical coordinates
m	axial mode number	(R,θ,ϕ)	spherical coordinates
n	circumferential mode number		
p_i	interior pressure	*Subscripts*	
p_r	far-field radiated pressure	e	exterior fluid
P_0	complex monopole source amplitude	i	interior fluid
q	acoustic mode number		